Wi-Sleep: Contactless Sleep Monitoring via WiFi Signals

Xuefeng Liu,Jiannong Cao
Dept. of Comp.
The Hong Kong PolyU
{csxfliu,csjcao}@comp.polyu.edu.hk

Shaojie Tang
Jindal School of Management,
University of Texas at Dallas
shaojie.tang@utdallas.edu

Jiaqi Wen
Dept. of Comp.
The Hong Kong PolyU
csjqwen@comp.polyu.edu.hk

***Abstract*—Is it possible to leverage WiFi signals collected in bedrooms to monitor a person's sleep? In this paper, we show that with off-the-shelf WiFi devices, fine-grained sleep information like a person's respiration, sleeping postures and rollovers can be successfully extracted. We do this by introducing Wi-Sleep, the first sleep monitoring system based on WiFi signals. Wi-Sleep adopts off-the-shelf WiFi devices to continuously collect the fine-grained wireless channel state information (CSI) around a person. From the CSI, Wi-Sleep extracts rhythmic patterns associated with respiration and abrupt changes due to the body movement. Compared to existing sleep monitoring systems that usually require special devices attached to human body (i.e. probes, head belt, and wrist band), Wi-Sleep is completely contactless. In addition, different from many vision-based sleep monitoring systems, Wi-Sleep is robust to low-light environments and does not raise privacy concerns. Preliminary testing results show that the Wi-Sleep can reliably track a person's respiration and sleeping postures in different conditions.**

I. Introduction

It is well recognized that sleep not only affects the productivity or physical vitality of a person, but also is related to many diseases including diabetes, obesity and depression [1]. Some sleep disorders such as the sleep apnea syndrome (OSAS), can even cause stroke and heart failure. On the other hand, although about one third of adults have suffered from poor sleep quality, most of them may not be able to evaluate their own sleep very well [2]. Therefore, a system which is able to provide quantitative sleep information is highly desirable.

To date, there are a large number of sleep monitoring systems, ranging from clinic standard Polysomnography (PSG) [3], to numerous commercial products [4][5][6]. In most of these systems, people usually need to wear some devices (e.g. wristbands, headband, and probes), to collect data that are used directly or indirectly to infer the sleep quality. These systems are more or less obtrusive to the users. In addition, many systems only provide coarse-grained sleep quality information (e.g. total sleep time). Sometimes, even this information can be biased since it is inferred from in-direct measurements (e.g. accelerations). The obtrusiveness to users, the coarse granularity, and the accuracy of results are among the major problems in many existing sleep monitoring systems.

Correspondingly, many non-obtrusive systems have been proposed recently. Most of these systems rely either on the pressure sensor arrays embedded in a mat and belt, or rely on vision and sounds. Systems using pressure sensor arrays, such as [7][8], can provide fine-grained sleep quality information like body motion, respiration, heart rate etc., but incurs high cost (e.g. the price of the Tanita Sleep Scan [8] is over 500US-D). The vision-based systems such as [9] and [10], however, may raise serious privacy concerns, and they may also be negatively affected by typically low-light sleep environments. More recently, there is an interesting sleep monitoring system called as iSleep [11], which uses the built-in microphone of the smartphone to detect the events that are closely related to sleep quality. However, key challenge in the iSleep is that the acoustic profile of sleep varies significantly from person to person. Moreover, the environmental noise can also affect the accuracy of detecting sleep-related events.

In this paper, we address those challenges by considering the following question: can we build a sleep monitoring system that (1) is completely non-obtrusive, (2) is capable of providing fine-grained sleep information with high accuracy, (3) incurs low cost, and (4) works well in a wide range of environmental conditions?

It is well known that the communication between two wireless devices can be affected by the presence or movement of a person nearby. This property has been utilized to determine the number of people in a room, their relative locations [12] [13], and even the possible gestures [14]. These successful applications of using wireless signals do shed some lights on us: *can we take wireless signals collected in a bedroom to monitor a person's sleep?* Even more aggressively, can we obtain some fine-grained sleep quality information such as a person's respiration?

The answer is surprisingly positive. We illustrate that by using off-the-shelf WiFi devices deployed in bedrooms, some fine-grained information associated with sleep including *the persons respiration*, *sleeping postures* and *activities like rollovers*, can be continuously tracked. Based on these findings, we propose Wi-Sleep, the first sleep monitoring based on WiFi signals. Wi-Sleep continuously collects the wireless channel state information (CSI) of the radio signals and from which extracts rhythmic patterns associated with breathing and abrupt changes due to body movement. Compared with existing works for sleep monitoring, Wi-Sleep is completely contactless, incurs low cost and is robust to low-light environments.

1052-8725/14 $31.00 © 2014 IEEE
DOI 10.1109/RTSS.2014.30

II. Tracking respiration using WiFi Radio : Preliminary findings and results

It is well known that the communication between two wireless devices can be affected by the presence or movement of a person nearby. This property has been utilized in [15][12][13][14] for device-free localization (i.e. to localize a person who does not carry any devices). For example, the authors in [15] leverage motion-induced variance of received signal strength indicator (RSSI) measurements to determine the location of a person. In [12], the RSSI variance caused by moving objects is utilized to track the location of a person or object behind walls. In [13], a device called Wi-Vi is proposed, which uses Wi-Fi OFDM signals in the ISM band (at 2.4 GHz) and typical Wi-Fi hardware to identify the number of people in a closed room and their relative locations. In [14], a system called WiSee is proposed, which enables even gesture recognition in line-of-sight, non-line-of-sight, and through-the-wall scenarios.

However, using wireless signals to monitor a person's sleep, particularly, to continuously track the respiration is much more challenging. It is well known that accompanied with breathing is the movement of a person's chest and abdomen, but whether such subtle movements could still be detected by analyzing the signal change? If so, which wireless feature is capable of fulfilling that task? Whether the respiration can be tracked under different sleeping positions, even with comforters? In this paper, we try to seek the answers to these questions.

A. Using ambient wireless signals for respiration detection, the first attempt

Which wireless feature is capable of tracking respiration? To answer this question, we start with some proof-of-concept experiments. We set up an experiment, in which two MicaZ node are deployed, one as the transmitter (TX) and the other one as the receiver (RX). TX and RX are with 3 meters apart from each other. A person is lying on a bed in between the TX-RX pair, breathing normally at approximately one breath (an inhalation-exhalation cycle) every 3 seconds. The TX keeps sending 100 packets per second at 1mW transmission power. From the received packets at RX side, we extract some wireless features and try to find out how they would change with time. Here, three mostly adopted wireless features are utilized: (1) received signal strength indicator (RSSI); (2) link quality indicator (LQI); and (3) packet loss rate (PLR). Note that since PLR is a statistical quantity measuring the packet loss in a period of time, here each PLR value is calculated using data collected within a one-second window. In the meantime, we attach a smartphone on the chest of the person to track the chest movement using the embedded accelerometers. This data will be taken as the ground truth of respiration.

Fig. 1 shows the testing results. From top to bottom, the four subfigures show how the acceleration, the RSSI, the LQI, and the PLR change over time. Unfortunately, it can be seen that there is no clear link between the rhythmic pattern shown in the acceleration data and any of the three wireless features (although for the RSSI, some patterns of breathing seem to be observed after 25 seconds). We then tried different location of the RX and TX and with different transmission power, but obtained similar results as shown in Fig. 1. These conventional wireless features seem not be able to well capture the minute activities like chest movement of a person.

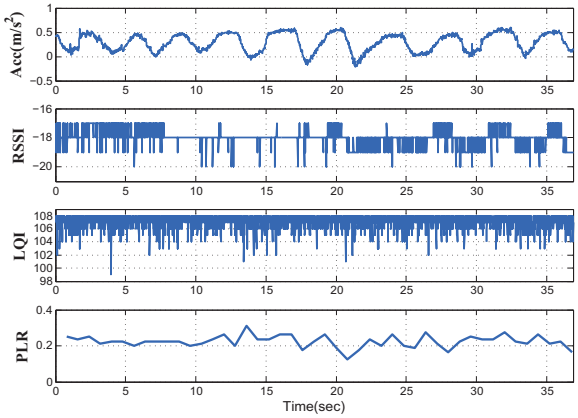

Fig. 1: Using conventional wireless features for tracking respiration. From top to bottom (a) the acceleration data (as the ground-truth) (b) the RSSI data (c) the LQI, and (d) the packet loss rate (PLR).

The main problem for these features is their low sensitivity and low resolution. Take the RSSI shown in Fig. 1 as an example. The RSSI values are integers, and when the person is breathing, the RSSI only changes within the range between -20 to -17. This coarse-grained RSSI values are reflected as stair-like pattern in Fig. 1 and hence they cannot capture the respiration well. However, the fact that 'the RSSI recorded after 25 seconds shows some respiration pattern' does inspire us: if we can find some wireless feature which has high sensitivity and resolution, then it is possible to capture the minute chest movement.

Then we turn our attention to Channel State Information (CSI) which has gained much attention in wireless communications recently [16]. CSI represents fine-grained PHY layer information that describes the channel property of a radio frequency (RF) link over the 30 subcarriers. CSI describes how an RF signal propagate from the TX(s) to the RX(s) and reveals the combined effect of, for instance, scattering, fading, and power decay with distance. CSI has gained popularity in a couple of applications, particularly in crowd counting [17] (i.e. to estimate the number of human beings within a region), and indoor localization [18].

These successful applications do enlighten us on utilizing CSI for tracking a person's respiration, and this will be explored in the next section.

B. CSI for tracking respiration

We start with some proof-of-concept experiments using CSI. We create a setup shown in Fig. 2 in an office at PolyU. We adopt one 802.11 compliant AP (TP Link WR740) as the TX and a laptop computer (Dell M2300) using a commercial 802.11n NIC as the RX. Note that here the NIC of the laptop has three antennas, and we extended all of them to outside

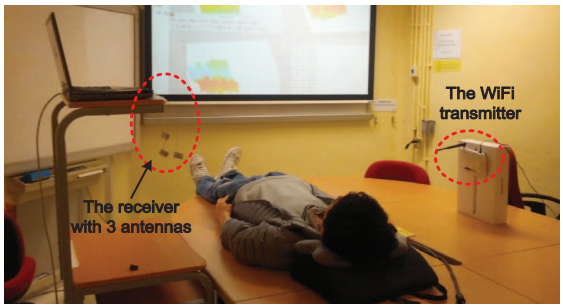

Fig. 2: Experiment setup using the CSI

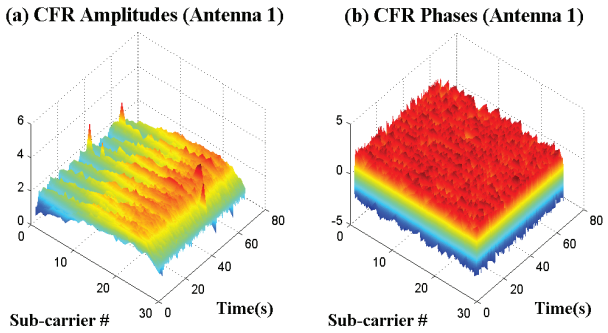

Fig. 3: The CFR amplitude and phase obtained during the experiment (antenna 1)

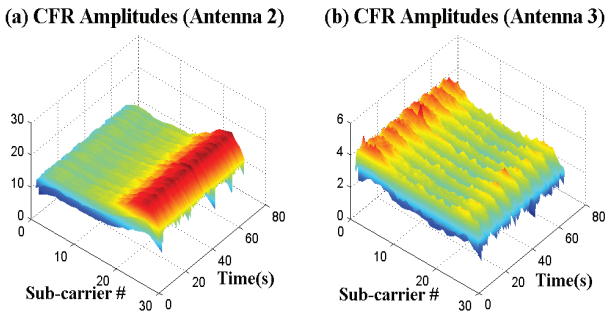

Fig. 4: The CFR amplitudes from antenna 2 and 3

(see 'the receiver with 3 antennas) for better signal quality. The TX sends 20 packets per second.

From each packet received from RX, we can extract a 30-by-3 matrix called as channel frequency response (CFR) matrix. Each column of the CFR matrix corresponds to one antenna while each row corresponds to one sub-carrier. Let $CFR^j(k)$ denote the j^{th} column of the matrix extracted from the k^{th} packet received:

$$CFR^j(k) = [h_1^j(k), h_2^j(k), \cdots, h_{30}^j(k)]^T, \quad (1)$$

where $h_i^j(k)$ is the CFR on the i^{th} subcarrier at time instant k of antenna j. Note that $h_i^j(k)$ is a complex number and is represented by the amplitude $|h_i^j|$ and the phase δh_i^j as $h_i^j = |h_i^j| * e^{j\delta h_i^j}$

To analyze the change of $CFR^j(k)$ with time, we put $CFR^j(k)$ received at different time together, denoted as CFR^j:

$$CFR^j = [CFR^j(1), CFR^j(2), \cdots, CFR^j(m)] \quad (2)$$

Note that CFR^j is a 30-by-m matrix, where m is the number of packets received. Each row of CFR^j represents the temporal change of the CSI information over one subcarrier.

Fig. 3 shows the amplitude and phase of CFR^1, using data collected during 70 seconds. From the amplitudes of CFR^1, we can clearly observe some ripple-like pattern, which we will shown soon corresponds to the movement of chest. On the other hand, the phase of the CFR^1 seems to be random and does not show clear correlation with breathing. Likewise, Fig. 4 shows the amplitudes of CFR^2 and CFR^3. The breathing-caused ripples can also be clearly observed at least for CFR^3.

To see whether these ripples are caused by the person's chest movement, we select the CFR sequence from the tenth row from CFR^1 (i.e. the time history of the CSI information of antenna 1 at the 10^{th} subcarrier). Fig. 5 compares the CFR sequence with the acceleration data recorded in the meantime. It can be seen that they exhibit strong correlation with each other.

C. Rational of using CSI for tracking a person's respiration

In this section, we try to give some intuition about why the CSI is capable of tracking subtle movement of chest. Ideally, a wireless signal would travel directly in a straight line from its transmitter to its intended receiver. This type of propagation is known as LOS (line-of-sight). However, when an obstacle stands in a signal's way, NLOS (non-line-of-sight) occurs and the signal can be subject to reflection, diffraction, and scattering. This is the well-known multipath propagation phenomenon. Obviously, during LOS and NLOS, the signal received by the receiver will have different CSI values (i.e. CRF). As shown in Fig. 6 (a), if, for example, the chest movement can cause a continuously shifting between LOS and NLOS, then the CSI values will show ripple-like pattern since the energy in the received packets via LOS and NLOS paths are significantly different.

However, in most conditions (including the scenario shown in Fig. 2), subtle chest movement can hardly keep generating such a shifting between LOS and NLOS. From the transmitter to the receiver, there is always a LOS path and a number of

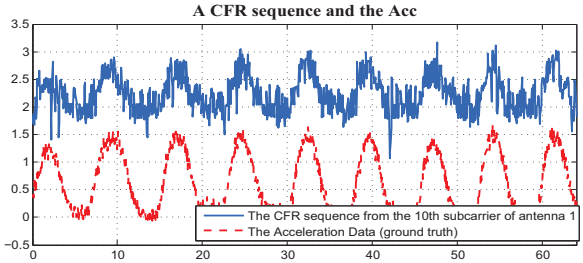

Fig. 5: A comparison of a CFR time history and the chest movement

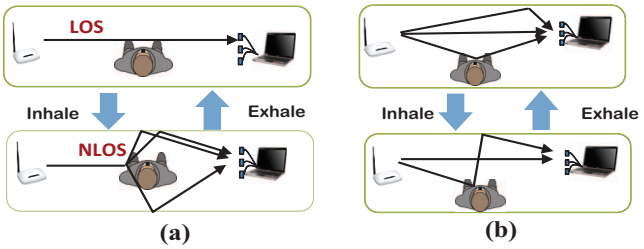

Fig. 6: Rationale of using CSI for respiration detection (a) Breathing causes change of communication paths between LOS to NLOS (b) Breathing causes change of communication of some NLOS paths.

NLOS paths. When a person is breathing, the chest movement will cause the change of some NLOS paths (as shown in Fig. 6 (b)). Different from the RSSI and LQI, CSI can describe how a RF signal from a transmitter propagates, via LOS and NLOS paths, to the receiver at the subcarrier level. Therefore, with the rhythmic movement of chest, the CSI values (e.g. the CFR^j) will show the ripple-like pattern.

III. Sleep Monitoring using WiFi Radio : Advanced findings and results

In the previous section, we describe some initial results when CSI is utilized to track a person's respiration. However, the scenario shown in Fig. 2 is somewhat idealistic. We summarize a few questions that deserve in-depth study.

(1) **The CSI data processing**. How to process the obtained CFR sequences such that a person's respiration can be reliably tracked? In particular, how to automatically select the best CFR sequences? (These questions will be addressed in Section III-A).

(2) **The effect of sleeping position**. The person shown in Fig. 2 was laying on his back with arms at his side. Whether sleeping position of a person affect the performance of using CSI? If so, how to handle it? (These questions will be addressed in Section III-B and III-C).

A. CFR data processing

In this section, we describe how the CFR can be processed for tracking respiration better. For example, as can be seen in Fig. 3(a) and Fig. 5, the collected CFR signals contain many outliers and heavy noise. How to handle these outliers and noise? In addition, we need to find a way to select the most appropriate subcarrier for tracking chest movement.

Outlier removal

The first step to process a CFR sequence is to remove outliers. We found that in the collected CFR sequences, there are some abrupt changes of CFR amplitudes that are obviously not caused by the movement of chest. Fig. 7(a) shows the CFR from all the 30 subcarriers of antenna 1. It can be seen that near 22s, 28s and 30s, there are some significant abrupt change of the CRF in some or all the subcarriers. We can also see some similar change points in Fig. 3. These are outliers for tracking chest movement and must be eliminated.

We utilize the Hampel identifier [19], which declares any point falling out of the closed interval $[\mu - \gamma * \sigma, \mu + \gamma * \sigma]$) as an outlier, where μ and σ are the median and the median absolute deviation (MAD) of the data sequence, respectively. The reason why we choose median and MAD instead of commonly used mean and standard deviation is because the latter two parameters are extremely sensitive to the presence of outliers in the data. γ is application dependent and the most widely used value is 3. We apply Hampel identifer on all the 30 subcarriers. Fig. 7(b) shows the results after all the identified outliers have been removed. We can see that the Hampel identifier performs very well in this scenario.

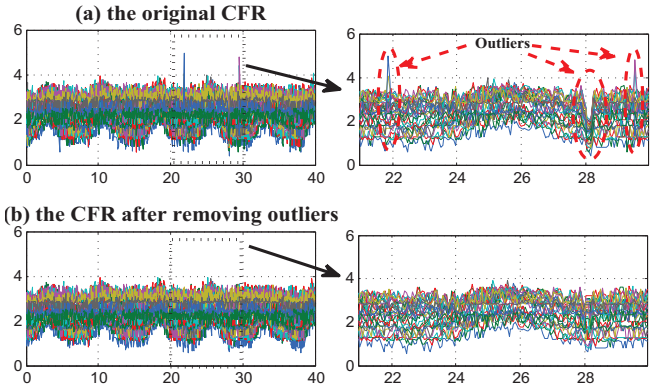

Fig. 7: (a)The original CRF from all the 30 subcarriers of antenna 1. Left: all the time span (from 0∼40 seconds, Right: selected time span(from 20 ∼ 30 seconds (b) The CRF after the outliers are removed using the Hampel filter.

Interpolation

It should be noted that in our previous experiment, although the transmitter is programmed to transmit packets every 50ms, we cannot guarantee the receiver is able to get one packet with the same frequency. We found that sampling jitter is quite common and sometimes can reach more than 300ms. Jitters are caused by packet loss, or due to the Linux system on the APs which lacks support for the users to arbitrarily prioritize high-level tasks. Therefore, the CFR signal must be interpolated. We utilize linear interpolation to obtain the CFR samples at the a universe sequence of evenly spaced time points, with 50ms apart between consecutive values.

Noise filtering

After interpolation, the noise contained in the CFR data should be eliminated. We argue that it is not appropriate to use conventional filters (e.g. the Butterworth and Chebyshev filters) to remove high frequency noise contained in the CFR. This is because they not only smooth away noise but also blur the rising/falling edges that possibly appeared in CFR signals, which is however critical for detecting sleep apnea and rollovers. Here, we apply the wavelet filter proposed in [20] since it can preserve extremely well the sharp transitions in signals than the other low-pass filters . To be more specific, we apply 4-level 'db4' wavelet transform on each CFR sequence and use only the approximation coefficients to 're-construct' the filtered signal. As an illustration, Fig. 8 (a) and (b) show all the 30 CFR sequences before and after using the wavelet

filtering. It can be clearly seen that the original noisy CFR signals becomes much cleaner.

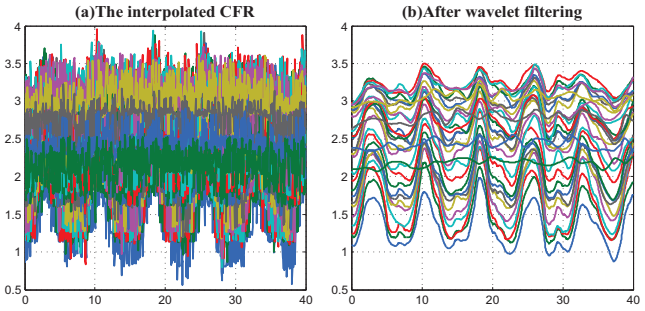

Fig. 8: (a) The interpolated 30 CFR sequences before using the wavelet filter (b) After using the wavelet filter.

Subcarrier selection

From the 30 CFR sequences, each corresponding to one of the 30 subcarriers, we will select the most appropriate one for tracking respiration. As can be seen from Fig. 8(b), not all the CFR sequences show the pattern of breathing. For example, Fig. 9 (a) show 5 CFR sequences from subcarriers $\#1, \#5, \#15, \#25, \#30$. We can see that some of CFR sequences, particularly for subcarrier $\#30$ (signal shown in the middle of Fig. 9(a)), do not contain as much information of breathing as others. Intuitively, we should select *a CFR sequence that has a high level of periodicity since in most conditions, the movement of chest shows rhythmic patterns*.

To quantify the periodicity of a time sequence X = $[x(1), x(2), \cdots, x(n)]$, we first find out its recurrence plot (RP) [21]. The RP depicts the collection of pairs of times at which the trajectory X gets sufficiently close to each other. Mathematically speaking, recurrence/non-recurrence can be recorded by the binary function

$$R(i,j) = \begin{cases} 1 & \text{if } ||x(i) - x(j)|| < \epsilon \\ 0 & \text{if otherwise,} \end{cases} \tag{3}$$

and the recurrence plot puts a (black) point at coordinates (i, j) if $R(i, j) = 1$.

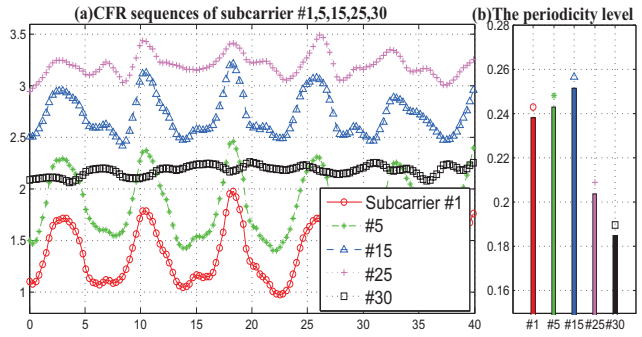

Fig. 9: (a)The CFR sequences from subcarrier $\#1, \#5, \#15, \#25, \#30$ (b) The corresponding periodicity level of the five CFR sequences.

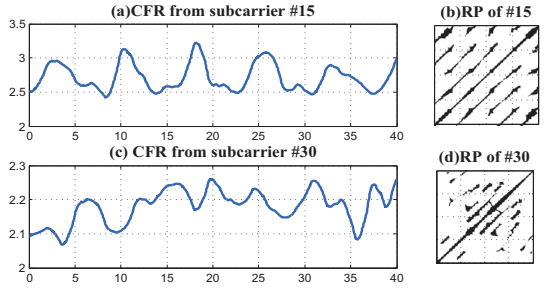

Fig. 10: (a)The CFR sequences from subcarrier $\#15$, (b) The recurrence plot of the CFR from $\#15$, (c) The CFR sequences from subcarrier $\#30$, (b) The recurrence plot of the CFR from $\#30$.

A recurrence plot makes it instantly apparent whether a signal is periodic or chaotic. For instance, if the sequence is strictly periodic with period T, then all such pairs of times will be separated by a multiple of T and visible as diagonal lines in the recurrence plot. On the other hand, a Gaussian process has totally chaotic-like recurrence plot. As an example, Fig. 10 shows clearly that the recurrence plot of $\#15$ is rather homogenous with many short, equally spaced diagonal lines, compared to that of $\#30$. This is the feature indicating that $\#15$ is 'more periodic' than $\#30$.

Having obtained the RPs, we rotate these RPs by 45^o and then apply the Singular Value Decomposition (SVD) on the rotated image. The periodicity of an RP, denoted as p_r, is the ratio of the largest singular value, denoted as λ_0, to the summation of all the singular values

$$p_r = \lambda_0 / \sum_i \lambda_i \tag{4}$$

The higher the p_r, the more periodic of the corresponding signal.

As an illustration, Fig. 9(b) depicts the value of p_r of the five CFR sequences shown in Fig. 9(a). It can be seen that the CFR sequences from the first three subcarriers (i.e. $\#1, \#5, \#15$) have higher p_r than the remaining two. This corresponds to the observation that the CFR sequences from the these three subcarriers look more periodic than others.

Fig. 11(a) shows the periodicity level of all the 30 CFR sequences shown in Fig. 8(b). It can be seen that $\#13$ has the highest p_r and is therefore selected. Fig. 11(b) shows the selected CFR and the acceleration data recorded at the same time. Note that for better comparison, the amplitude of the acceleration data is standardized. It can be seen that using the selected CFR can accurately track the chest movement.

At last, it should be noted that the respiration is monitored in a real-time manner. The collected data are first stored in a fix-sized buffer, and when the buffer is full, the CFR sequences are processed to obtain the respiration information and then the buffer is emptied. The buffer size is dependent on the requirement of users. In this paper, 200 is utilized. Considering the sampling frequency of CSI is 20Hz, we can provide sleep information every 10 seconds.

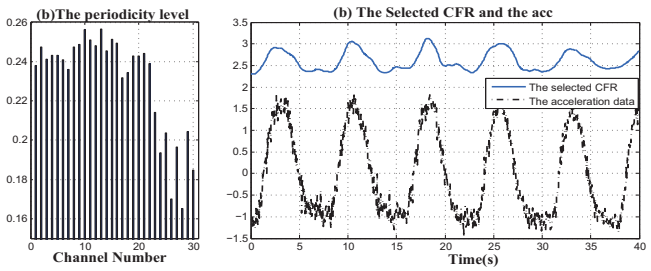

Fig. 11: (a)The periodicity level of 30 CFR sequences (b) The selected CFR subcarrier (i.e. Subcarrier #13) and the acceleration data.

In this real-time monitoring scenario, selecting subcarrier is not implemented each time when the buffer is full. Instead, we found that we can simply select the previously selected subcarrier as long as the person does not change his sleeping positions. The detecting changes of sleeping position will be described in Section III-C.

B. The effect of sleeping positions

In the experiment shown in Fig. 2, the person was laying on his back with arms at his side. In this section, we will study the effect of different sleeping positions.

Fig. 12 shows 6 most common sleeping positions [22]:

- Foetus : Sleeping all curled up into a ball with knees drawn up and chin tilted down.
- Log: On side, arms at sides.
- Yearner: On side, arms out.
- Soldier : On back, arms at sides.
- Freefaller: Face down.
- Starfish :On back, arms up.

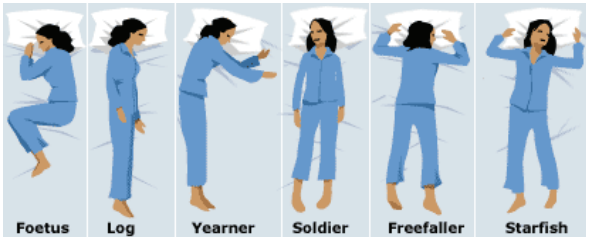

Fig. 12: The most popular sleeping positions. From left to right: Foetus, Log, Yearner, Solider, Freefaller, and Starfish. (The figure is from [22]).

We test the performance of the system when the person is at different sleeping positions. In particular, the TX and the RX are placed at two sides of the person (as shown in Fig. 2) and the person is breathing normally for about 10 minutes.

As an example, Fig. 13(a) shows, when the person is in the 'Foetus' position, the processed CFR sequences of all the 30 subcarriers in a 30-second period. Fig. 13(b) shows the finally selected CFR and corresponding acceleration data. Similarly, Fig. 13(c) and (d) show the corresponding results of the 'Starfish' position. Obviously, the respiration can be much better tracked when the person is using 'Starfish' than the 'Foetus'.

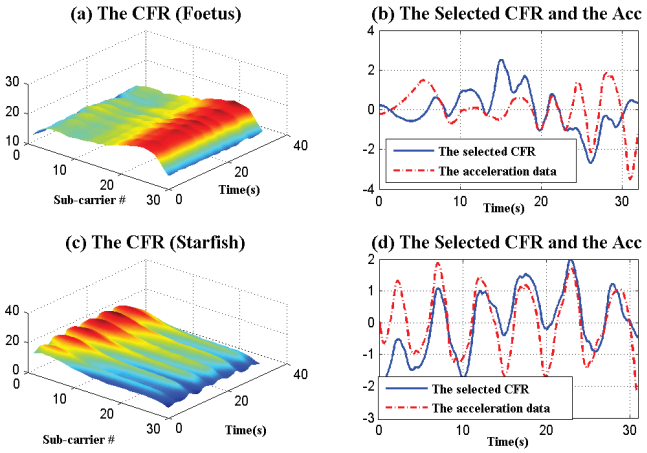

Fig. 13: The results of the system for sleeping positions 'Foetus' and 'Starfish'. (a) the CFR sequences of 30 subcarrier (after pre-processing) for 'Foetus' (b) the selected CFR sequence and the acceleration data. (c) and (d) the results for 'Starfish'.

What causes the problem? After a thorough study, we found that it is caused by the 'mis-match' between the location of the TX-RX pair and the person's sleeping position. In these experiments, the TX and the RX are placed at different side of the human body. As shown in Fig. 14 (a), for the sleeping positions like the 'Soldier' and 'Starfish' in which the person is facing upward, there are many NLOS paths that carry information of the chest movement. These *'effective paths'* are generated when the wireless signal sent from the TX is reflected from the chest. In this condition, respiration can be well captured using the CSI information. However, for the 'Foetus', 'Log', and 'Yearner' in which the person is sleeping on one side (see Fig. 14(b)), the number of effective paths is much smaller, and the performance will be degraded.

To be able to better track the chest movement under 'Foetus', 'Log', and 'Yearner', we need to change the position of the TX-RX pair such that the number of effective paths can be increased. This can be achieved by placing both the TX and the RX at the same side of the human chest, as shown in Fig. 14 (c).

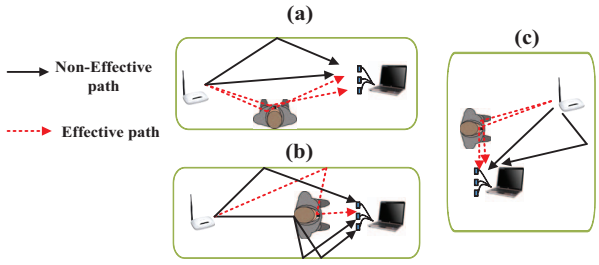

Fig. 14: (a)For sleeping positions like the 'Soldier' and 'Starfish', there are many effective paths which carry information of chest movement (b) For sleeping positions like 'Foetus', 'Log', and 'Yearner', the number of 'effective paths' is much smaller. (c) By changing the positions of the TX-RX pair, the number of effective paths can be increased.

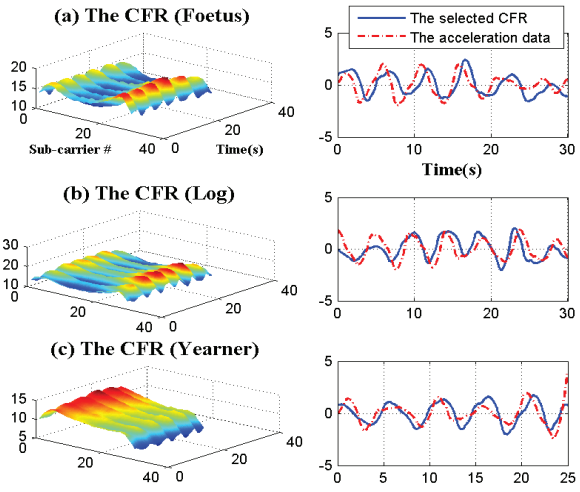

Fig. 15: The results of the system for sleeping positions 'Foetus','Log', and 'Yearner'.

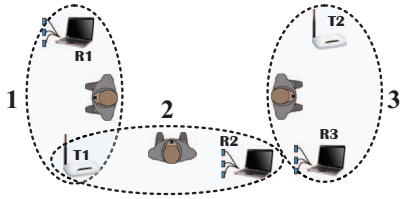

Fig. 16: Three pairs of TX-RX collaboratively work to monitor the respiration of a person with different sleeping positions. Transmitter 1 (T1) and Receiver 1 (R1) work when the person is sleeping on his left side. T1-R2 work when the person is sleeping on his back, and T2-R3 are utilized for the right-side sleeping positions.

As an illustration, Fig. 15 (a), (b), and (c) show results of sleeping positions 'Foetus', 'Log', and 'Yearner', respectively. It can be seen that with change of the location of the TX-RX pair, the performance of the system is significantly improved.

Therefore, we argue that to be able to reliably track a person's breathing, three pairs of wireless TX-RX are needed. As shown in Fig. 16, the first pair, consisting of transmitter 1 (T1) and the receiver 1 (R1), is placed at the left side of a person to track his respiration when he is sleeping on his left side. The second pair, T1-R2, is utilized when he was sleeping on his back. Note that these two pairs share the same T1. This can be achieved by letting T1 broadcast WiFi signals that can be received by both R1 and R2. The third pair T2-R3, is placed at the right side of the person to track the respiration when he was sleeping at the right side. It should be noted that we cannot eliminate R3 by letting R2 alternatively receive WiFi signals from T1 and T2 because the handoff usually takes a few seconds.

In practical condition, the actual sleeping position of a person is not known a priori. How to select the most appropriate TX-RX pair without known the person's sleeping posture? The basic idea is that we choose the pair which generates 'the most periodic CFR sequence'. This idea is similar to selecting a subcarrier from 30 CSI sub-carriers that has been described in Section III-A. The details of this part will be described in the next section.

C. Detecting change of sleeping positions

In this section, we will answer the following question: Given the CFR data from three pairs of TX-RX, how one's sleeping position can be identified? For simiplicity, instead of identifying 6 sleeping positions shown in Fig. 12, we classify those 6 positions into three categories: 'sleeping on one's back', 'sleeping on one's left side' and 'sleeping on one's right side'. Identifying sleeping positions is important because this information not only helps us to select the most appropriate TX-RX pair for tracking respiration, but also directly provides information like rollovers, which is associated with sleep quality.

We start from an experiment in which the person shown in Fig. 2 changed sleeping positions a few times as follows:

1) Initially, he slept *on his back* (from $0 \sim 82$ seconds), then he turned over and
2) slept *on his left side* (from $83 \sim 110$ seconds), and he turned over again and
3) slept *on his back* (from $111 \sim 148$ seconds), and he turned over again and
4) slept *on his right side* (from $149 \sim 175$ seconds), and finally he turned over and
5) slept *on his back* (from $176 \sim 201$ seconds)

Following the procedures described in Section III-A, Fig. 17 shows the obtained CFR sequences from TX-RX pairs T1-R2, T1-R1, and T2-R3, respectively. Note that these CFR sequences are standardized. We can see that the CFR from T1-R2 gives a good indication of respiration during $0 \sim 80s$, $110 \sim 145s$,$175 \sim 200s$, which matches very well with the time slots when the person was sleeping on his back. On the other hand, T1-R1 tracks respiration well during $80 \sim 110s$, corresponding to the time when the person was sleeping on his left side. For T2-R3, we can see that its CFR sequence clearly shows the trace of respiration only when the person was on the right side (i.e. during $145 \sim 175s$). These observations match well with our previous discussion that different TX-RX pair should be adopted for different sleeping positions.

Now we will identify sleeping positions using the CFR sequences shown in Fig. 17. The basic idea is to compare the periodicity level of the three CFR sequences and the TX-RX pair with the highest periodicity level will be utilized to determine the sleeping position. More specifically, we first divide each CFR sequence into a number of sections. The length of each section is 10 seconds. Then for each section, we calculate the periodicity level as described in Section III-A. Fig. 18 shows the periodicity level of all the 20 sections for T1-R2, T1-R1, and T2-R2. It can be seen that for the first 8 sections (which correspond to $0 \sim 80s$), the periodicity level of T1-R2 is the highest, and therefore the person should be sleeping on his back during the period. For sections $\#9 \sim \#11$ (which correspond to $80 \sim 110s$), T1-R1 has the highest level, we conclude that during this period, the person should be sleeping on his left side. In the similar way, the

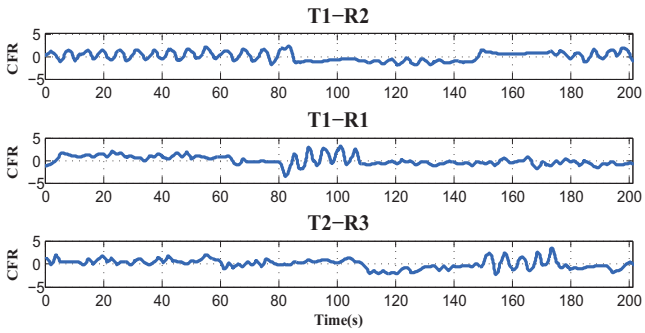

Fig. 17: The processed CFR sequences from T1-R2, T1-R1, and T2-R3, respectively. It can be seen that T1-R2 gives a better indication of respiration when the person is sleeping on his back. On the other hand, T1-R1 and T2-R3 can track respiration well when the person is sleeping on his left and right sides, respectively

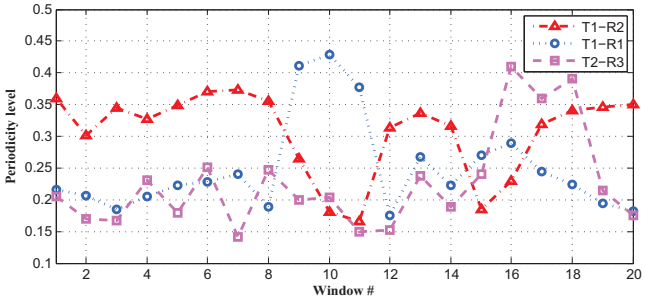

Fig. 18: The periodicity level of the CFR sequences from T1-R2, T1-R1, and T2-R3, respectively. For the first 8 sections, T1-R2 has the highest value among the three and therefore, the person should be sleeping on his back. From section 9 to 11, T1-R1 has the highest periodicity levels and therefore, the person should be sleeping on his left side. The other sleeping positions can also be identified in the similar way.

remaining sleeping positions can be correctly identified. Given the sleeping positions, the rollovers can be directly obtained.

IV. Experiments

In this section, some preliminary results of our system will be described. More specifically, we will evaluate our system in two aspects: (1) the capability of the system to track respiration of a person with fixed sleeping positions, and (2) the capability of the system to identify sleeping positions.

A. Quantifying identification errors

Before we show the results, we briefly describe how to quantitively evaluate the result of respiration tracking. Given the processed CFR sequence and the ground-truth acceleration data, as every cycle in the CFR sequence corresponds to a respiratory cycle, we utilize location of peaks identified in the acceleration data and in the CFR sequences to evaluate the results. The basic idea is that for each peak in the acceleration signal, if there exists a peak in the CFR sequence occurring at the same time, then we say that a correct respiration is identified. Otherwise, there are either 'false positives' and 'false negatives'.

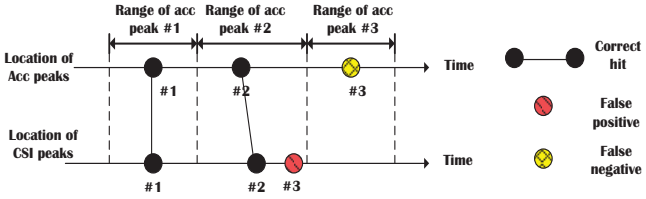

Fig. 19: An example to calculate false positives and false negatives of using peaks identified from the acceleration data and from the CFR sequence.

More specifically, let T_{CFR} and T_{ACC} denote the locations of peaks identified in the CFR sequence and the acceleration signal, respectively:

$$T_{CFR} = [t_1, t_2, ..., t_n], T_{ACC} = [\tau_1, \tau_2, ...\tau_m], \quad (5)$$

where t_i and τ_j are the locations of peaks identified from the CFR sequence and from the acceleration data, respectively. First, we should note that due to the noise and difference in the peak shapes, even a cycle of respiration is correctly identified, the corresponding peaks in T_{CFR} and T_{ACC} generally do not occur at the same time. Therefore, we first define an effective range for each of the peaks location in T_{ACC}. For τ_i, its effective range is defined as $[\tau_i - \frac{\delta\tau_i}{2}, \tau_i + \frac{\delta\tau_{i+1}}{2}]$, and $\delta\tau_i = \tau_i - \tau_{i-1}$ is the distance between τ_{i-1} and τ_i.

For each peak location $\tau_i \in T_{ACC}$, if there exsit at least one corresponding peak location in T_{CFR} that falls in the effective range of τ_i, then we have *a correct hit*. On the other hand, if we find there are p ($p > 1$) elements in T_{CFR} in the range of τ_i, we conclude that there are $p-1$ *extra hits*, representing $p-1$ false positives. When there is no peak in T_{CFR} in the range of τ_i, then we call it *a missing hit*, which is a false negative. Let n^+ are n^- are the total number of false positives and false negatives in the given data, we calculate the false positive and negative ratios, denoted as P^+ and P^-, respectively as follows:

$$P^+ = n^+/N, P^- = n^-/N, \quad (6)$$

where N is the number of peaks for the acceleration data.

Fig. 19 uses an example to illustrate this. Here we have three elements for both T_{ACC} (top) and T_{CFR} (bottom). Firstly, we find out the ranges for the three elements in the T_{ACC}. Obviously, for the first two elements in T_{ACC}, there is a 'correct hit' in the T_{CFR}. However, there is one false positive for the second element in T_{ACC} and a false negative for the last element in T_{ACC}.

B. Experimental results

Experiment setup:

We set up the experiment similar like the one shown in Fig. 2 but with two differences. Besides the TX-RX pair, denoted as T1-R2 shown in the figure, we place (1) an extra laptop (R1) at right side of the person, and (2) an extra TX-RX pair (T2-R3) at the left side of the person. The transmitter T1 is programmed to broadcast packages to R1 and R2 every 50ms, and T2 is programmed to send pacakges to R3 with the same

rate. The data will be processed by the corresponding laptop. In the meantime, the ground-truth respiration is obtained by a smartphone attached to the person's chest.

Tracking respiration with fixed sleeping positions

We first test the system's performance when the person is at fixed sleeping positions shown in Fig. 12. For each position, the test lasts about 4 minutes. For convenience, we let the person always sleep at his left side for positions including 'Foetus', 'Log' and 'Yearner'. Therefore, only data from T1-R2 (which is placed at different side of the person) and from T1-R1 (which is placed at the left side of the person) will be utilized in this experiment.

Fig. 20(a) shows the false positive ratio P^+ and false negative ratio P^- using CFR sequences from T1-R2. It can be seen that when the person is sleeping on his back (e.g. 'Soldier' and 'Starfish'), T1-R2 performs very well. The false positives and false negatives are lower than 5%. However, when the person is sleeping at one side, using T1-R2 will obtain relatively high P^+ and P^- (up to 27%).

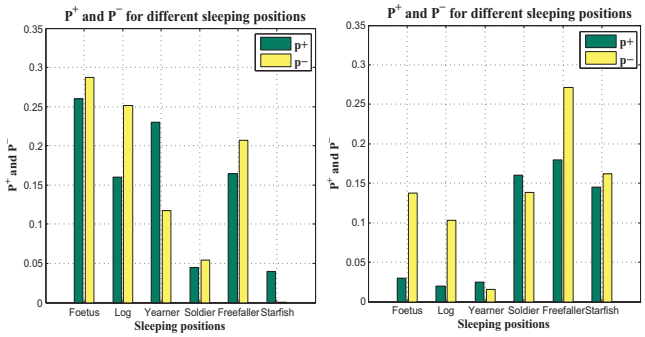

(a) Using data from T1-R2 (b) Using data from T1-R1

Fig. 20: The false positive and negative ratios under different sleeping positions using CSI data from T1-R2 and T1-R1, respectively. The results show that using data from T1-R2, the respiration can only be tracked well when the person is sleeping on his back (i.e. 'Soldier' and 'Starfish'), while using data from T1-R1 can work well when the person is sleeping on one side (i.e. 'Foetus','Log', and 'Yearner').

On the other hand, Fig. 20b shows the results using data from T1-R1. We can see that using data from T1-R1, the person's respiration can be accurately monitored for 'Foetus', 'Log', and 'Yearner'. The results match well with our observations described in Section III-B. Therefore, if we can accurately identify whether the person is sleeping on his back or on one side, we can expect that using the correpsonding TX-RX pair can achieve a good result of tracking respiration.

It should be noted that the system seems not be able to track the respiration of a person with 'Freefaller' position, even with different placement of TX-RX pairs. We believe the reason is because with this position, the respiration can only cause very slight movement of the back, which is too weak to be identified in the CSI signals. However, we believe that with the widespread of WLAN, the bandwidth of CSI can be significantly improved. With Fine-grained CSI, detecting respiration under 'Freefaller' could be easier.

Type of changing positions	Total times	Correctly identified times	Sucessful rate(%)
A → B	12	10	83.3
B → A	12	11	91.6
A → C	10	8	80
C → A	10	9	90
B → C	8	8	100
C → B	8	7	87.5

TABLE I: The summary of changes of positions in the test

Identifying change of postions

We test the performance of the system to identify a person's sleeping positions. For convience, we define three different positions as A, B, and C, respectively:

- A : Sleeping on the back
- B : Sleeping on the left side
- C : Sleeping on the right side

The test last for 15 minutes, and during which the test subject changed his sleeping positions for a totoal of 60 times. These change of postions can be dividied into 6 categories: A→B, B→A, A→C, C→A, B→C and C→B. For each cateogry, the number of changes are shown in the second column of Table I. In this experimet, the person stayed in a postion for about $20 \sim 30s$, and then turned over quickly (in approximately 1 second) to another one.

Table I also shows the number of correctly identified position changes and the sucessful rate. It can be seen that using the method proposed in Section III-C, we can reliably detect whether a person is sleep on his back/left side/right side. The detection error is less than 20%.

V. Related Works

We categorize the related works into two parts, those related to sleep monitoring, and those related to using wireless radios to identify human activities.

A. Sleep monitoring

It is well known that although PSG [3] can provide detailed information about one's sleep, it is obtrusive to the patients and requires expensive equipments. To address this problem, many 'less-obtrusive' sleep monitoring products are designed. Usually, people need to wear some devices such as wristbands [4][5], headband [6], or probes [23], to collect data that are used directly or indirectly to infer the sleep quality.

Recently, many sleep monitoring systems emerge that are totally unobtrusive. For example, [11] uses the built-in microphone of the smartphone to detect the events that are closely related to sleep quality, including body movement, couch and snore, and infers quantitative measures of sleep quality. However, the system can be affected by noise in the environment. Some systems rely on a specially designed sheet or belt put on the bed to monitor the sleep condition [7] [8]. These systems usually incur high cost.

Another type of unobtrusive sleep monitoring systems rely on video cameras to monitor sleep via sleep posture patterns and breath patterns [24][9][25][10]. However, using video can

suffer from typically low-light sleep environments and raises privacy concerns for users.

B. Human activity detection using wireless signals

Recently, there are some research attempt of using wireless raido as a sensing tool to detect human locations and activities. For example, [12] utilizes the received signal strength (RSS) variance caused by moving objects to track the location of a person or object behind walls. In [13], a device called Wi-Vi is proposed, which uses Wi-Fi OFDM signals in the ISM band (at 2.4 GHz) and typical Wi-Fi hardware to identify the number of people in a closed room and their relative locations. [14] proposes WiSee, a system that enables gesture recognition in line-of-sight, non-line-of-sight, and through-the-wall scenarios. WiSee extracts minute Doppler shifts from wide-band OFDM transmissions and from which to infer human gestures. However, these works only can identify relatively large activities of a person.

Perhaps the most related work to us is the one proposed in [26], which leverages the RSSI information collected from directional antennas to estimate the breathing rate. However, as we have illustrated in Section II-A, using the CSI can obtain much richer information than using the RSSI. In addition, we have demonstrated the effectiveness of Wi-Sleep for different sleeping positions, while in [26], only the 'Soldier' position is tested.

VI. Conclusion and future work

In this paper, we introduce how to take WiFi signals collected in bedrooms as 'sensors' to monitor a person's sleep. The preliminary results show that with off-the-shelf WiFi devices, fine-grained sleep information like a person's respiration, sleeping postures and rollovers can be reliably extracted.

There are still many interesting problems that deserve in-depth study. For example, can the CSI help to identify activities like getting-ups or hand movements? Can we still be able to track the respiration of a person in the presence of these activities? What is the minimum transmission power that we can set without decreasing the system's performance of tracking a person's sleep? Can we monitor multiple persons simultaneously? What is the performance of the system for different persons, and in different room environment? How to place the TX-RX pairs such that the performance of the system can be optimal? We are working on these questions and hope to obtain some satisfactory results in near future.

VII. Acknowledgment

This research is financially supported in part under RGC General Research Fund B-Q28G, Germany/HK Joint Research Scheme 3-ZG2S, and the NSF of China with Grant 61332004.

References

[1] F. P. Cappuccio and et al., "Quantity and quality of sleep and incidence of type 2 diabetes a systematic review and meta-analysis," *Diabetes care*, vol. 33, no. 2, pp. 414–420, 2010.

[2] http://www.springerreference.com/docs/html/chapterdbid/345724.html.

[3] C. A. Kushida and et al., "Practice parameters for the indications for polysomnography and related procedures: an update for 2005," *Sleep*, vol. 28, no. 4, pp. 499–521, 2005.

[4] "Sleep tracker." http://www.sleeptracker.com/.

[5] "Fitbit." http://www.fitbit.com/.

[6] J. R. Shambroom and et al., "Validation of an automated wireless system to monitor sleep in healthy adults," *Journal of Sleep Research*, vol. 21, no. 2, pp. 221–230, 2012.

[7] J. Paalasmaa, M. Waris, H. Toivonen, L. Leppakorpi, and M. Partinen, "Unobtrusive online monitoring of sleep at home," in *Engineering in Medicine and Biology Society (EMBC), 2012 Annual International Conference of the IEEE*, pp. 3784–3788, 2012.

[8] "Tanita." https://www.tanita.co.jp/products/models/sl501.html/.

[9] W.-H. Liao and C.-M. Yang, "Video-based activity and movement pattern analysis in overnight sleep studies," in *Pattern Recognition, 2008. ICPR 2008. 19th International Conference on*, pp. 1–4, 2008.

[10] "Philips vital signs camera." http://www.vitalsignscamera.com/.

[11] T. Hao, G. Xing, and G. Zhou, "isleep: unobtrusive sleep quality monitoring using smartphones," in *The 11th ACM Sensys*, p. 4, 2013.

[12] J. Wilson and N. Patwari, "See-through walls: Motion tracking using variance-based radio tomography networks," *IEEE Transactions on Mobile Computing*, vol. 10, no. 5, pp. 612–621, 2011.

[13] F. Adib and D. Katabi, "See through walls with wi-fi!," in *ACM SIGCOMM*, 2013.

[14] Q. Pu and et al., "Whole-home gesture recognition using wireless signals," in *ACM MobiCom*, pp. 27–38, 2013.

[15] M. Moussa and M. Youssef, "Smart cevices for smart environments: Device-free passive detection in real environments," in *IEEE PerCom*, pp. 1–6, IEEE, 2009.

[16] Z. Yang, Z. Zhou, and Y. Liu, "From rssi to csi: Indoor localization via channel response," *ACM Computing Surveys (CSUR)*, vol. 46, no. 2, p. 25, 2013.

[17] W. Xi and et al., "Electronic frog eye: Counting crowd using wifi,"

[18] K. Wu, J. Xiao, Y. Yi, M. Gao, and L. M. Ni, "Fila: Fine-grained indoor localization," in *IEEE INFOCOM*, pp. 2210–2218, 2012.

[19] L. Davies and U. Gather, "The identification of multiple outliers," *Journal of the American Statistical Association*, vol. 88, no. 423, pp. 782–792, 1993.

[20] J. D. Villasenor and et al., "Wavelet filter evaluation for image compression," *IEEE Transactions on Image Processing*, vol. 4, no. 8, pp. 1053–1060, 1995.

[21] J.-P. Eckmann and et al., "Recurrence plots of dynamical systems," *EPL (Europhysics Letters)*, vol. 4, no. 9, p. 973, 1987.

[22] http://news.bbc.co.uk/2/hi/health/3112170.stm.

[23] J. Zhang, D. Chen, J. Zhao, M. He, Y. Wang, and Q. Zhang, "Rass: A portable real-time automatic sleep scoring system," in *IEEE 33rd Real-Time Systems Symposium (RTSS)*, pp. 105–114, 2012.

[24] K. Nakajima and et al., "A monitor for posture changes and respiration in bed using real time image sequence analysis," in *Engineering in Medicine and Biology Society*, vol. 1, pp. 51–54, 2000.

[25] C. Scully and et al., "Physiological parameter monitoring from optical recordings with a mobile phone," *IEEE Transactions on Biomedical Engineering*, vol. 59, no. 2, pp. 303–306, 2012.

[26] O. J. Kaltiokallio, H. Yigitler, R. Jäntti, and N. Patwari, "Non-invasive respiration rate monitoring using a single cots tx-rx pair," in *Proceedings of the 13th international symposium on Information processing in sensor networks(IPSN 2014)*, pp. 59–70, 2014.